Characterization of star forming regions in (U)LIRGs

D. Miralles-Caballero[1,2], L. Colina[1,2], P. E. Belles[3], P. A. Duc[3], S. Arribas[1,2], and F. Bournaud[3]

[1] Instituto de Estructura de la Materia (IEM/CSIC), c/ Serrano 121, 28006 Madrid, Spain
[2] Departamento de Astrofísica, Centro de Astrobiología, CSIC-INTA, Ctra. de Torrejón Ajalvir km 4, Torrejón de Ardoz, 28850 Madrid, Spain
[3] Laboratoire AIM, CEA, CNRS Université Paris Diderot, Irfu/Service dAstrophysique CEA-Saclay, 91191 Gif sur Yvette Cedex, France

Abstract

A statistical analysis of almost 3000 star forming regions (knots) in a representative sample of 32 (U)LIRGs has been performed by means of high angular resolution ACS/HST B and I images. We present the results of the photometric characterization of these star forming regions as a function of the infrared luminosity of the systems (we have split the sample in three luminosity bins) and the interaction phase (four interaction phases have been defined). Properties such as sizes, colors and luminosities are compared with those of clusters observed in less luminous interacting galaxies and the state-of-the-art models of major mergers.

1   Introduction

During the last two decades massive young compact clusters have been discovered and studied in different environments (e.g. [1, 9, 21, 2, 13]). With masses of 10^4–10^6 M$_\odot$ and sizes around 5 pc (in terms of r_{eff}), most of these objects are identified as Young Massive Clusters (YMCs), and have been proposed as progenitors of the old globular clusters in galaxies. However, little is known about the formation and evolution of stellar clusters in Luminous (LIRG; L_{IR}[1] $= 11$–12) and Ultraluminous (ULIRG; $L_{\mathrm{IR}} = 12$–13) Infrared Galaxies, representing the most extreme cases of starbursts and interactions in our nearby Universe (e.g. [17, 5, 4, 6, 20]).

Establishing the general properties of the star clusters in (U)LIRGs as a function of luminosity and interaction phase would provide relevant information in order to understand the mechanisms that govern the formation and evolution of star-forming galaxies. Previous

---

[1]We identify $L_{\mathrm{IR}}(\mathrm{L}_\odot) = \log(L_{\mathrm{IR}}[8\text{–}1000\mu\mathrm{m}])$

studies have been mainly focused only on small samples of ULIRGs. Thus, no study has been done so far on a representative sample of luminous infrared galaxies covering the different phases of the interaction process as well as the entire LIRG and ULIRG luminosity range. This paper presents the first attempt at obtaining an homogeneous and statistically significant study of the photometric properties (magnitudes, colors and sizes) of optically-selected clusters found in these systems as a function of $L_{\rm IR}$, morphology (i.e interaction phase) and radial distance to the nucleus of the galaxy. Additional data from a state-of-the-art high linear resolution numerical simulation of a major merger [3] and the use of synthesis stellar population techniques will help us understand such properties.

2 The sample and data

Galaxies were selected from the flux-limited IRAS Revisited Galaxy Sample (RBGS, [15]) and [14], using the following additional criteria: to sample the wide range of IR luminosities in (U)LIRGs, to cover all types of nuclear activity, to span different phases of interaction and to optimize the linear scales by selecting low-z galaxies.

Our sample comprises 32 low-z systems, 20 LIRGs and 12 ULIRGs. It is not complete either in volume, flux or luminosity. However, this sample is essentially representative of the local (U)LIRG systems: (1) it covers the luminosity range $11.39 \leq L_{\rm IR} \leq 12.54$ and the redshift range $0.016 \leq z \leq 0.124$ (from 65 to about 550 Mpc), with the median value 0.037; (2) it spans all types of nuclear activity, with different excitation mechanisms such as LINER (i.e., shocks, strong winds, weak AGN), HII (star formation) and Seyfert-like (presence of an AGN); and (3) all the different morphologies usually identified in these systems are also sampled.

The results presented here are based on high angular resolution archival HST images. Advanced Camera for Surveys (ACS) broad-band images were taken for thirty systems from the Hubble Legacy Archive (prop ID 10592, PI Evans), with the filters F814W and F435W. For IRAS 13536+1836 and IRAS 15206+3342, Wide Field Planetary Camera 2 (WFPC2) images were taken (prop ID 5982, PI Sanders), with the filters F814W and F439W. The pixel size in both instruments corresponds to about $0.05''$.

3 Results

3.1 Properties of the knots as a function of $L_{\rm IR}$

In order to investigate whether the properties of the star-forming knots do show a dependence with the infrared luminosity (i.e. star formation rate), we have divided the initial sample in three $L_{\rm IR}$ intervals. We aim at covering the low, intermediate and high luminosity regimes while preserving a similar number of systems per luminosity bin for the subsequent statistical analysis. We have therefore chosen the following luminosity intervals: $L_{\rm IR} < 11.65$ (low), $11.65 \leq L_{\rm IR} < 12.0$ (intermediate) and $L_{\rm IR} \geq 12.0$ (high). The number of systems that lie in each interval are 11, 9 and 12, being at an average distance of 99, 166 and 258 Mpc,

respectively. For each L_{IR} bin, we have excluded the knots of systems located at the two extremes of the distance scale, in order to diminish distance effects within the intervals. A summary of the properties of the knots per luminosity bin is given in Table 1.

Table 1: Photometric properties of the sample as a function of L_{IR}

L_{IR}	knots per system	$<D_L>$ (Mpc)	$<M>$ F814W	$<M>$ F435W	$<C>$	$< r_{eff}^I >$ (pc)	α LF F814W	α LF F435W
$L_{IR} < 11.65$	113 ± 102	99 ± 26	-11.37	-10.14	1.12	25	1.83 ± 0.02	1.78 ± 0.02
$11.65 \leq L_{IR} < 12.0$	84 ± 59	178 ± 27	-12.74	-11.85	0.80	55	1.93 ± 0.03	1.95 ± 0.03
$L_{IR} \geq 12.0$	38 ± 15	246 ± 72	-14.09	-12.97	0.97	81	1.87 ± 0.02	1.86 ± 0.02

Notes. The values betwen brackets ($<>$) correspond to the median value of the distribution of the observable considered. Magnitudes (M), the color M_{F435W}-M_{F814W}(C), sizes (r_{eff}) and the slope of the LF (α) are given.

The fact that ULIRGs are intrinsically further away (the measurements suffer from a distance effect) can explain some of the differences shown in the table. We have studied this effect by degrading the images corresponding to the first L_{IR} interval as if they were a factor of 2.6 further (distance ratio of low and high luminosity interval systems). Taking into account distance effects, knots in ULIRGs are still more luminous by a factor of 4–5 than in low luminous LIRGs. If we assume an statistically similar extinction and age for the star-forming knots regardless of the L_{IR} of the system, the most plausible explanation for the luminosity excess measured in the intermediate and high luminosity systems has to invoke a mass and/or density effects:

- Mass effect, i.e. the mass of the knots increases intrinsically with the infrared luminosity of the system.

- Density effect, i.e. the knots are aggregates of an intrinsically larger number of clusters as the infrared luminosity of the system increases.

With the available data it is hard to disentangle if one or the combination of the two effects is taking place. Another interesting result is that the slope (α) of the luminosity function (LF) remains close to a value of 2, like in other less luminous interacting galaxies such as in NGC 3921, NGC 7252, NGC 4038/39, M51, etc [16, 12, 21, 7].

3.2   Properties of the knots as a function of interaction phase

Most of the systems in our sample are interacting systems, hence we have divided the sample in four groups, depending on the morphology seen in the F814W HST images, using a merging classification scheme similar to that given by [19]. Each group represents snapshots of the different phases of the interaction/merger: first approach (category I-II), pre-merger (III), merger (IV) and post-merger (V). In order to diminish distance effects we study those systems located at similar distances, in the range 75–180 Mpc.

Table 2: Photometric properties of the sample as a function of interaction phase

Interaction phase	Number of systems	knots per system	$<D_L>$ (Mpc)	$<M>$ F814W	$<M>$ F435W	$<C>$	$<r^I_{\rm eff}>$ (pc)	α LF F814W	α LF F435W
First Approach	3	153 ± 127	121 ± 49	-11.25	-10.26	0.93	24	1.69 ± 0.03	1.68 ± 0.02
Pre-merger	8	145 ± 81	126 ± 42	-11.91	-10.78	1.06	35	1.84 ± 0.03	1.87 ± 0.04
Merger	6	139 ± 123	107 ± 37	-11.23	-10.24	0.96	22	1.97 ± 0.05	1.86 ± 0.03
Post-Merger	5	34 ± 19	145 ± 50	-13.35	-11.49	1.49	44	1.94 ± 0.03	1.96 ± 0.02

Notes. Same notation as in Table 1.

3.2.1 SSC merging scenario?

The knots in the post-merger phase are significantly more luminous (median *I*-band magnitude difference of up to 2 magnitudes), and redder than in any of the three earlier phases (see results in Table 2). Besides, the population of knots in the post-merger phase shows in its color distribution an extension towards redder colors (> 3 mag), which implies that the knots there are more obscured or older. If they were more extinct, then the difference in luminosity would be even greater. If they were older, they would fit in an evolutionary scenario proposed by [8]. Accordingly, many dozens or even hundreds of massive individual star clusters with masses of 10^5–10^7 M$_\odot$ could merge into super star clusters (SSCs) after few hundred Myr. As the interaction progresses, the smaller SSCs would be destroyed by disruption effects and few young massive clusters (YMCs) would still be able to form. Thus, in the post-merger phase systems we might be detecting only the evolved, more massive and larger SSCs and a few YMCs.

3.2.2 Evolution of the LF with the interaction?

There appears to be a trend in the slopes of the LF with the interaction phase such that they become steeper as the interaction evolves from first contact to pre-merger and up to merger and post-merger phases (slopes of 1.69, 1.84, 1.97 and 1.94, respectively, with the red filter).

In order to investigate this further we have compared the characteristics of the observed knots with those detected in a numerical model of a major merger [3] with a linear resolution in the range of the observed one. In the simulation the merger is monitored and a total of 78 snapshots are obtained from $t = 39$ Myr to $t = 1053$ Myr, in steps of 13 Myr. Each snapshot provides information on the mass and position of each particle. Sources (simulated knots) were then identified using an algorithm based on particle counts and extracted above a S/N with respect to the local background. Using the magnitude-color evolutionary tracks of stellar synthesis population (SSP) models and knowing the age of the simulated knots, photometric magnitudes were computed. For population younger than 100 Myr the tracks for the SB99 model [10, 18] were used and for older population the Maraston model [11] was considered since it applies a rigorous treatment of the thermally pulsing asymptotic giant branch.

We identify in the simulation typical ages for the pre-merger, merger and post-merer interaction phases to be 299, 585 and 988 Myr, covering each an age range of about 150

Table 3: Slopes of the mass and luminosity distributions of the simulated and observed knots at different interaction phases.

Interaction phase	N_Y (%)	$\alpha_{LF\ F814W}$	$\alpha_{LF\ F814W}$ sim50	$\alpha_{LF\ F435W}$	$\alpha_{LF\ F435W}$ sim50
pre-merger	17 ± 9	1.65 ± 0.05	1.86 ± 0.06	1.70 ± 0.05	1.92 ± 0.06
merger	4 ± 2	1.82 ± 0.05	1.91 ± 0.05	1.76 ± 0.05	1.92 ± 0.05
post-merger	1 ± 1	1.85 ± 0.04	1.82 ± 0.04	1.82 ± 0.04	1.83 ± 0.04

Notes. The value given for the slope of the LF represents the average of the median values of the slopes computed for the 11 distributions per interaction phase. N_Y gives the number of young simulated knots (i.e. age $\leq$ 50 Myr) with respect to the total number of simulated knots. "sim50" refers to the results of the simulated data when only knots older than 50 Myr have been considered.
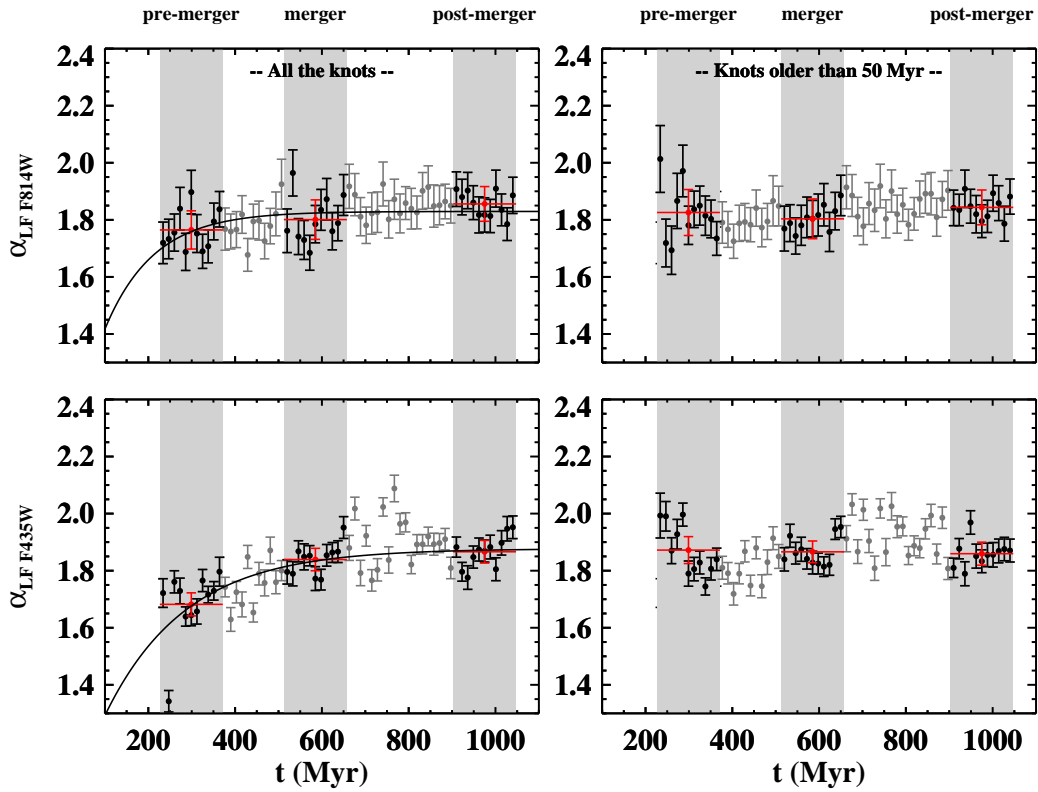

Fig. 1: Computed slope of the LF for filter F814W (top) and F435W (bottom) of the simulated knots as the interaction evolves. The shaded areas mark the time period, identified with the different interaction phases, for which the median value of the slopes enclosed has been computed in each case (in red). The line shows the best fit of the function $\alpha_{LF} = -10^{\beta t/t_0} + c$.
.

Myr. We have then fitted the LF of the simulated knots per snapshot, using all the knots and only knots older than 50 Myr (see Fig. 1 and Table 3). The LFs of the observed knots follow a similar behavior than the LFs of the simulated knots, in which there is a marginally significant indication that for the red filter it evolves during the interaction process. For the blue filter the slope does not change perceptibly. This evolution of the LF is not seen when we do the fit for the knots older than 50 My. This is an indication that in early phases the population younger than 50 Myr represents a higher fraction of the total population than in most evolved phases (see Table 3).

4   Concluding remarks

As we have seen, this study provides evidence that the formation and evolution of star clusters in (U)LIRGs depend both on the total luminosity of the galaxies and on the interaction phase. First, brighter knots (agrupation of more massive or larger number of clusters) are found in the most luminous systems. Additionally, there is also evidence of a dynamical evolution of the clusters (merging of SSCs and change in the shape of the LF) with the interaction.

Acknowledgments

References

[1] Barth, A. J., et al. 1995, AJ, 110, 1009

[2] Bik, A., Lamers, H. J. G. L. M., Bastian, N., Panagia, N., & Romaniello, M. 2003, A&A, 397, 473

[3] Bournaud, F., Duc, P., & Emsellem, E. 2008, MNRAS, 389, L8

[4] Bushouse, H. A., et al. 2002, ApJS, 138, 1

[5] Cui, J., Xia, X.-Y., Deng, Z.-G., Mao, S., & Zou, Z.-L. 2001, AJ, 122, 63

[6] Evans, A. S., Mazzarella, J. M., Surace, J. A., & Sanders, D. B. 2002, ApJ, 580, 749

[7] Haas, M. R., Gieles, M., Scheepmaker, R. A., Larsen, S. S., & Lamers, H. J. G. L. M. 2008, A&A, 487, 937

[8] Kroupa, P. 1998, MNRAS, 300, 200

[9] Larsen, S. S., & Richtler, T. 1999, A&A, 345, 59

[10] Leitherer, C., et al. 1999, ApJS, 123, 3

[11] Maraston, C. 2005, MNRAS, 362, 799

[12] Miller, B. W., Whitmore, B. C., Schweizer, F., & Fall, S. M. 1997, AJ, 114, 2381

[13] Peterson, B. W., Struck, C., Smith, B. J., & Hancock, M. 2009, MNRAS, 400, 1208

[14] Sanders, D. B., et al. 1988, ApJ, 325, 74

[15] Sanders, D. B., Mazzarella, J. M., Kim, D., Surace, J. A., & Soifer, B. T. 2003, AJ, 126, 1607

[16] Schweizer, F., Miller, B. W., Whitmore, B. C., & Fall, S. M. 1996, AJ, 112, 1839

[17] Surace, J. A., Sanders, D. B., Vacca, W. D., Veilleux, S., & Mazzarella, J. M. 1998, ApJ, 492, 116

[18] Vázquez, G. A., & Leitherer, C. 2005, ApJ, 621, 695

[19] Veilleux, S., Kim, D.-C., & Sanders, D. B. 2002, ApJS, 143, 315

[20] Veilleux, S., et al. 2006, ApJ, 643, 707

[21] Whitmore, B. C., et al. 1999, AJ, 118, 1551